RCWA and FDTD modeling of light emission from internally structured OLEDs

Michiel Koen Callens,[1,*] Herman Marsman,[2] Lieven Penninck,[1] Patrick Peeters,[2] Harry de Groot,[2] Jan Matthijs ter Meulen,[3] and Kristiaan Neyts[1]

[1]*ELIS Department, Ghent University, Sint-Pietersnieuwstraat 41, B-9000,Ghent, Belgium*
[2]*OM&T B.V., Moser Baer Technologies Europe, High Tech Campus 29, 5656 AE, Eindhoven, The Netherlands*
[3]*Lumiteq B.V., High Tech Campus 29, 5656 AE, Eindhoven, The Netherlands*
**michiel.callens@elis.ugent.be*

Abstract: We report on the fabrication and simulation of a green OLED with an Internal Light Extraction (ILE) layer. The optical behavior of these devices is simulated using both Rigorous Coupled Wave Analysis (RCWA) and Finite Difference Time-Domain (FDTD) methods. Results obtained using these two different techniques show excellent agreement and predict the experimental results with good precision. By verifying the validity of both simulation methods on the internal light extraction structure we pave the way to optimization of ILE layers using either of these methods.

OCIS codes: (160.4890) Organic materials; (230.3670) Light-emitting diodes; (050.1950) Diffraction gratings; (260.6970) Total internal reflection; (310.4165) Multilayer design; (240.0310) Thin films.

References and links

1. M. H. Lu and J. C. Sturm, "Optimization of external coupling and light emission in organic light-emitting devices: modeling and experiment," J. Appl. Phys. **91**(2), 595–604 (2002).
2. S. Möller and S. R. Forrest, "Improved light out-coupling in organic light-emitting diodes employing ordered microlens arrays," J. Appl. Phys. **91**(5), 3324–3327 (2002).
3. Y.-C. Kim, S.-H. Cho, Y.-W. Song, Y.-J. Lee, Y.-H. Lee, and Y. R. Do, "Planarized SiNx/spin-on-glass photonic crystal organic light-emitting diodes," Appl. Phys. Lett. **89**(17), 173502 (2006).
4. C. Fuchs, T. Schwab, T. Roch, S. Eckardt, A. Lasagni, S. Hofmann, B. Lüssem, L. Müller-Meskamp, K. Leo, M. C. Gather, and R. Scholz, "Quantitative allocation of Bragg scattering effects in highly efficient OLEDs fabricated on periodically corrugated substrates," Opt. Express **21**(14), 16319–16330 (2013).
5. Y. Sun and S. R. Forrest, "Enhanced light out-coupling of organic light-emitting devices using embedded low-index grids," Nat. Photonics **2**(8), 483–487 (2008).
6. M. G. Salt and W. L. Barnes, "Flat photonic bands in guided modes of textured metallic microcavities," Phys. Rev. B **61**(16), 11125–11135 (2000).
7. C. H. Chang, K. Y. Chang, Y. J. Lo, S. J. Chang, and H. H. Chang, "Fourfold power efficiency improvement in organic light-emitting devices using an embedded nanocomposite scattering layer," Org. Electron. **13**(6), 1073–1080 (2012).
8. J. W. Shin, D. H. Cho, J. Moon, C. W. Joo, S. K. Park, J. Lee, J. H. Han, N. S. Cho, J. Hwang, J. W. Huh, H. Y. Chu, and J. I. Lee, "Random nano-structures as light extraction functionals for organic light-emitting diode applications," Org. Electron. **15**(1), 196–202 (2014).
9. K. Yee, "Numerical solution of initial boundary value problems involving Maxwell's equations in isotropic media," IEEE Trans. Antenn. Propag. **14**(3), 302–307 (1966).
10. *Lumerical Solutions, Inc.* http://www.lumerical.com/tcad-products/fdtd/.
11. Kahnert and F. Michael, "Numerical methods in electromagnetic scattering theory," J. Quant. Spectrosc. Radiat. Transf. **79-80**, 775–824 (2003).
12. M. G. Moharam and T. K. Gaylord, "Rigorous coupled-wave analysis of planar-grating diffraction," J. Opt. Soc. Am. **71**(7), 811–818 (1981).
13. P. Bienstman, "CAMFR manual," version 1.3. http://camfr.sourceforge.net/docs/camfr.pdf.
14. P. Bienstman, "Rigorous and efficient modelling of wavelength scale photonic components," PhD thesis (2001).
15. K. A. Neyts, "Simulation of light emission from thin-film microcavities," J. Opt. Soc. Am. A **15**(4), 962–971 (1998).

#203447 - $15.00 USD Received 20 Dec 2013; revised 21 Feb 2014; accepted 26 Feb 2014; published 12 Mar 2014

16. S. Jeon, J.-W. Kang, H.-D. Park, J.-J. Kim, J. R. Youn, J. Shim, J.-H. Jeong, D.-G. Choi, K.-D. Kim, A. O. Altun, S.-H. Kim, and Y.-H. Lee, "Ultraviolet nanoimprinted polymer nanostructure for organic light emitting diode application," Appl. Phys. Lett. **92**(22), 223307 (2008).
17. Fluxim,"Setfos 3.2," Release 3.2.2657, http://www.fluxim.com.

1. Introduction

OLED lighting panels are both unique and compelling as light sources due to their ability to provide illumination over large surfaces, their ultra-thin composition and their capacity to be transparent and flexible. However, at their present developmental stage, OLED lighting panels have reduced brightness and have a high cost per lumen in comparison with LEDs and compact fluorescent lighting. This reduced brightness can be partly attributed to the fact that only around 20% of the light generated by the OLED can 'escape' it, while the majority is trapped due to total internal reflection at material interfaces and is subsequently lost by absorption within various layers. It is possible to extract light trapped inside waveguide modes using both external and internal light management layers. However, while External Light Extraction (ELE) layers have been extensively researched and are widely employed in industry [1,2], the integration and optimization of Internal Light Extraction (ILE) layers has proved to be more difficult, primarily as a result of electrically driven OLEDs' sensitivity to moisture, rough surfaces and small particles. Thus, experiments attempting to optimize light extraction structures and materials are time consuming and costly. An interesting alternative is to use software models to optimize the light management stack and feature sizes. These software models should allow for the simulation of sub-micrometer structures that are present in the vicinity of the emission zone. This requires solving Maxwell's equations in the given complex geometry for a light-emitting point source. In this article two different software models, using a different approach in solving Maxwell's equations, are compared mutually and with experimental data. This article is unique in the sense that it, in contrast to previous articles on the subject [3–6], combines accurate simulations of electrically driven internally structured OLEDs with experimental demonstrations and verifications.

The two software models under investigation are: Finite-Difference Time-Domain (FDTD) and Rigorous Coupled Wave Analysis (RCWA). The aim is to verify both software models for the OLED Internal Light Extraction (ILE) layer application, modeling a 2D diffractive groove structure. This analysis will consequently expedite more accurate results, faster optimization procedures and ultimately more efficient and cost effective OLED lighting panels. Besides the periodic structures under investigation in this work, there is also the possibility of embedding randomly structured layers within the OLED device. Even though these methods show promising results [7,8] they are difficult to simulate because of their lack of periodicity, which is why they will not be discussed further in this work.

2. Background

2.1 Finite difference time-domain method

The FDTD method is a numerical analysis technique used for solving Maxwell's equations in complex geometries. The time-dependent Maxwell's equations (in partial differential form) are discretized using central-difference approximations for the spatial and temporal partial derivatives. Since it is a time-domain method, FDTD simulations can cover a wide frequency range (by exploiting Fourier transform properties) with a single simulation run and handle nonlinear material properties in a natural way. In FDTD, space is discretized into box-shaped cells, which are small in comparison to the wavelength (see Fig. 1(a)).

The so-called cubic Yee cell [9] uses the following conventions: the electric field is defined at the edge centers of the cube; the magnetic field is defined at the face centers of the cube; the electric permittivity/conductivity is defined at the cube center and the magnetic permeability/magnetic loss is defined at the cube corners.

#203447 - $15.00 USD Received 20 Dec 2013; revised 21 Feb 2014; accepted 26 Feb 2014; published 12 Mar 2014

Time is quantized into small steps, where each step represents the time required for the field to travel from one cell to the next. The electric and magnetic fields are updated using a leapfrog scheme where first the electric, and then the magnetic fields are computed for each step in time. Light emission is then modeled by imposing a source current in a number of Yee cells. In this paper, a commercial-grade simulator based on the finite-difference time-domain method was used to perform the FDTD simulations [10]. For more information on the FDTD method (and other simulation methods) we refer to [11].

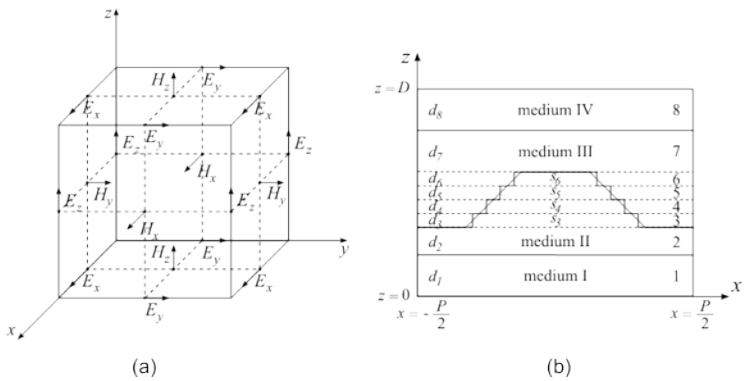

Fig. 1. (a) Yee cell used for FDTD simulations. (b) A staircase approximation of a trapezoid grating for RCWA modeling.

2.2 Rigorous coupled wave analysis

The Rigorous Coupled Wave Analysis (RCWA) method is a semi-analytical method in computational electromagnetics that is typically employed to solve diffraction of a field by a given periodic grating structure [12]. The devices and fields are represented by a sum of spatial harmonics, since RCWA is a Fourier-space method. In a uniform layer the spatial harmonics correspond to the well-known plane waves. The method is based on Floquet's theorem, which states that the solutions of periodic differential equations can be expanded in Floquet functions. A device is divided into a number of z-invariant layers. A staircase approximation is necessary for curved features (see Fig. 1(b)). Light emission is modeled by an elementary electrical dipole antenna embedded in one of the layers. The electromagnetic modes in each layer are calculated and analytically propagated through the layers. The overall problem is solved by matching boundary conditions at each of the interfaces between the layers using scattering matrices. Once modes in each of the layers are calculated these can be used as a new base for the electromagnetic radiation. The radiation pattern can then be projected on this new base, for which Maxwell's equations take an algebraic form. By cutting off higher-order Floquet functions, depending on the required accuracy and convergence speed, a finite system of algebraic equations is obtained, which can be solved numerically. In this paper, the simulation software CAMFR developed by Bienstman is used [13]. For more information on the RCWA method we refer to [14].

2.3 Analytical solution for planar OLEDs

For benchmarking the numerical simulations, we can use the analytical solution that is available for the coherent emission of an elementary dipole antenna in a stack of uniform layers [15]. In this method the dipole radiation is decomposed into plane (and evanescent) waves and a matrix method is used to express the boundary conditions at the interfaces between different layers. This analytical model is limited to planar (unstructured) OLEDs.

#203447 - $15.00 USD Received 20 Dec 2013; revised 21 Feb 2014; accepted 26 Feb 2014; published 12 Mar 2014

3. Methods: measurements and simulations

In this paper we study the effect of a 2D diffractive light extraction structure inside an OLED, by comparing numerical simulations with real devices. The device we consider is inspired by the work by Jeon et al. on an internal 3D diffractive structure [16].

3.1 OLED samples

OLED samples, with a 2D ILE layer, have been made by use of an imprint method. The master structure is first imprinted in a replication lacquer on glass (Corning Eagle XG). After curing the imprint lacquer this master structure is removed. The resulting structure with parallel grooves is shown in Fig. 2. The depth of the grooves is approximately 290 nm as measured on the imprint stamper. The groove width of the inverse sample has a FWHM of 260 nm and a pitch of 600 nm. The AFM picture shows that the grooves are not perfectly rectangular but rounded. In the simulations a structure layer thickness of 260 nm is used, accounting for shrinkage and rounded profile.

Subsequently, the structure is planarized with a high refractive index acrylic planarization lacquer (n = 1.8). This lacquer is applied by spin coating and cured thermally. Figure 3 shows a schematic representation of both the planar OLED (Fig. 3(a)) and the OLED with an ILE layer (Fig. 3(b)). The stack on which the OLED is deposited consists of a glass substrate with thickness 0.7 mm, a replication layer of 5 µm, a structure layer of 260 nm and planarization layer with negligible thickness.

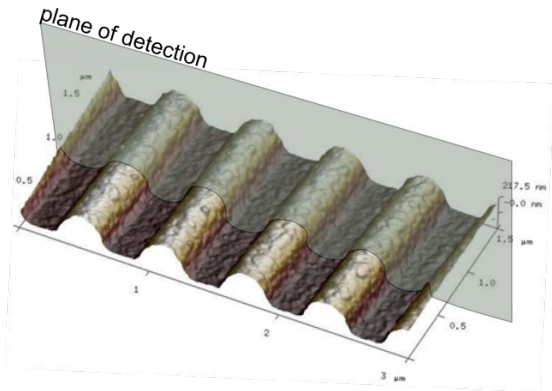

Fig. 2. AFM picture of the replicated structure on the substrate with indication of the plane of detection.

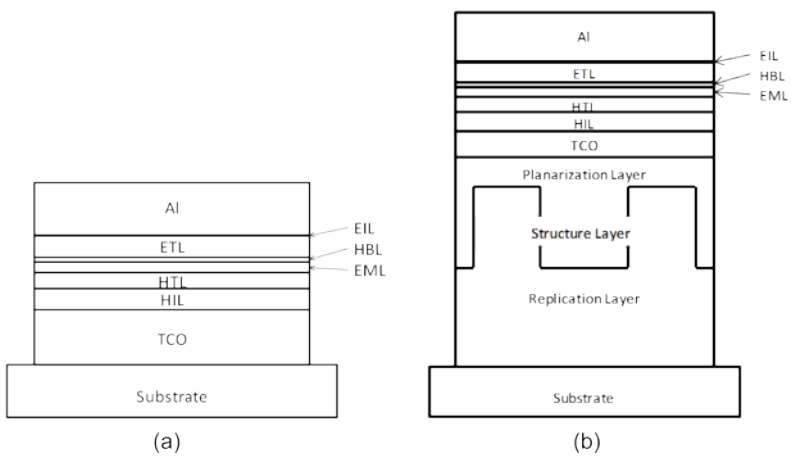

Fig. 3. (a) cross-section of the planar OLED. (b) cross-section of the OLED with ILE layer.

#203447 - $15.00 USD Received 20 Dec 2013; revised 21 Feb 2014; accepted 26 Feb 2014; published 12 Mar 2014

In the next step the OLED stack, based on a phosphorescent green emitter, is deposited. The same stack is applied, either directly on the glass (planar reference sample) or on the high refractive index planarization layer for the samples with an ILE layer. The Transparent Conductive Oxide (TCO) layer consists of sputtered Indium-Tin-Oxide (ITO) and has a thickness of 135 nm. Subsequently, the organic layers are evaporated: 40 nm Hole Injection Layer (HIL, material: LG-101), 30 nm Hole Transport Layer (HTL, material: NPB), 20 nm Emissive Material Layer (EML, materials: Host Merck TMM-100 + dopant Merck TEG-341 10%), 10 nm Hole Blocking Layer (HBL, material: Merck TMM-100), 40 nm Electron Transport Layer (ETL, materials: Merck ETM-036 + 50% LiQ) and 1 nm Electron Injection Layer (EIL, material: Lithium-Fluoride). Finally, the organic stack is covered with a 100 nm thick cathode layer of Aluminum (Al). The OLED stack is designed in such a way that the emission is restricted to the EML, which is necessary for a comparison with simulations. The OLED samples have a size of 2.6 x 2.8 cm^2. The fabricated OLED, with the ILE layer, shows diffractive effects when illuminated with a bright light (see Fig. 4).

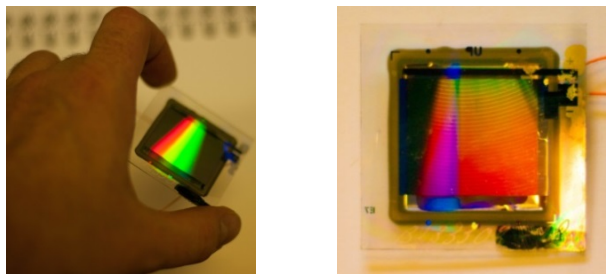

Fig. 4. Two photographs of an OLED with ILE layer showing iridescent reflections. The OLED sample has a size of 2.6 x 2.8 cm^2.

3.2 Measurement set-up

To compare the simulations with experimental results, the angular distributions of the emitted light from the planar OLEDs and the OLEDs with an ILE layer were measured. As the numerical simulations provide the emission pattern in the glass substrate of the OLED, a cylindrical lens is placed over the sample in such a way that the sample is in the center of the lens. By making use of an index matching fluid and a slit of 1 mm x 8 mm between the OLED and the lens, the light emitted into the substrate can be coupled out into air with the same intensity and angle of propagation as in the substrate. By using a cylindrical lens with a rectangular slit instead of a circular aperture in combination with a hemisphere lens we can increase the SNR significantly, when measuring under specific angles with a fine resolution. The samples are positioned with the grooves perpendicular to the plane of detection (see Fig. 5(a)). The detector itself is covered with a 1 mm diaphragm and the distance between the detector and the OLED center is approximately 100 mm. Light extracted from the OLED structure goes through some focusing optics into a fiber spectrometer with NA 0.1 . The focusing optics and the fiber input are mounted in a rotatable arm, which automatically relocates to the desired angles and measures the emitted spectrum. Figure 5(a) shows a schematic drawing of the set-up. Measurements are done for both positive and negative emission angles and the resulting symmetrical data is then used to sensitively calibrate the zero emission angle.

In a second measurement the total light output of the reference samples and of the sample with ILE layer were measured in an integrating sphere with an internal diameter of 10 inch (25.4 cm). The samples were measured with and without a hemisphere lens, to determine the light emission into the glass substrate and air respectively. A hemisphere lens, with a diameter of 65 mm, was attached to the OLED with an index matching fluid.

#203447 - $15.00 USD Received 20 Dec 2013; revised 21 Feb 2014; accepted 26 Feb 2014; published 12 Mar 2014

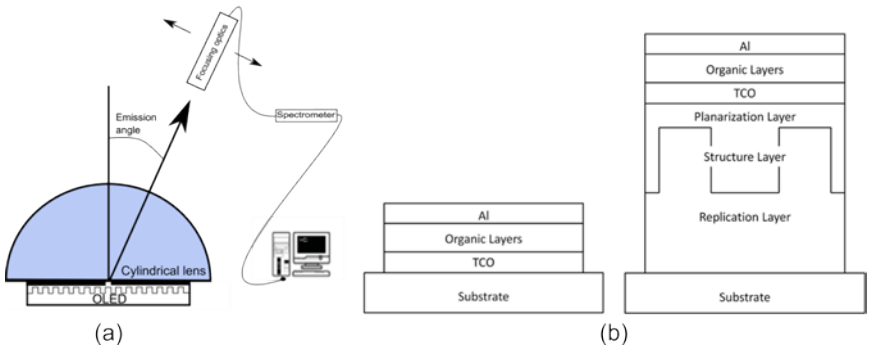

Fig. 5. (a) Schematic drawing of the experimental setup used for Angular Spectral Measurements (ASMs). (b) OLED devices as simulated. (left) Planar OLED, (right) OLED with ILE layer.

3.3 Software models

To compare the RCWA and FDTD models the two OLED devices shown in Fig. 5(b) are used. In these devices the organic layers are treated as one layer because the differences in optical parameters are relatively small. The optical parameters of aluminum are calculated using Fluxim [17] and are shown in Fig. 6(a). Apart from aluminum, the values for n and k used in simulations are based on experimental measurements using optical interferometry and are given in Fig. 6(b). In order to determine the real and imaginary part of the refractive index and the thickness of layers using optical interferometry we analyze the spectral content of the reflection and transmission of the stack. With this information we can fit the optical constants and thickness of the layers. The refractive indices at 500 nm are 1.51 for the substrate and 1.76 for the organic layers. The optical constants of the replication lacquer are identical to those of the glass substrate.

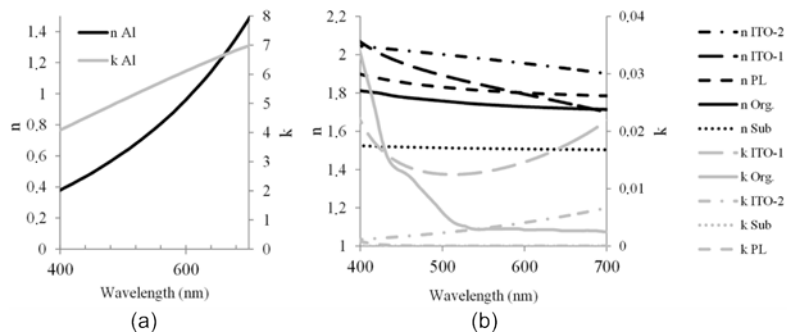

Fig. 6. (a) Wavelength dependency for the optical constants of Aluminum (Al) [17]. (b) Optical constants used in the model for the organic layer (Org.), the two fitted ITO layers, the planarization layer (PL) and the substrate (Sub).

Our experimental sputtered ITO has a graded index, which is taken into account in the simulations by splitting the ITO layer in two layers with slightly different refractive indices. The optical constants of the two layers (see Fig. 6 (b)) are determined by optical interferometry on planar ITO samples. Both sub layers of the ITO layer were simulated using two lorentz oscillators, one absorbing in IR and the other in UV. This gives us a good approximation of the optical behavior of this layer while keeping calculation times limited. The result of this fit is shown in Fig. 7.

#203447 - $15.00 USD Received 20 Dec 2013; revised 21 Feb 2014; accepted 26 Feb 2014; published 12 Mar 2014

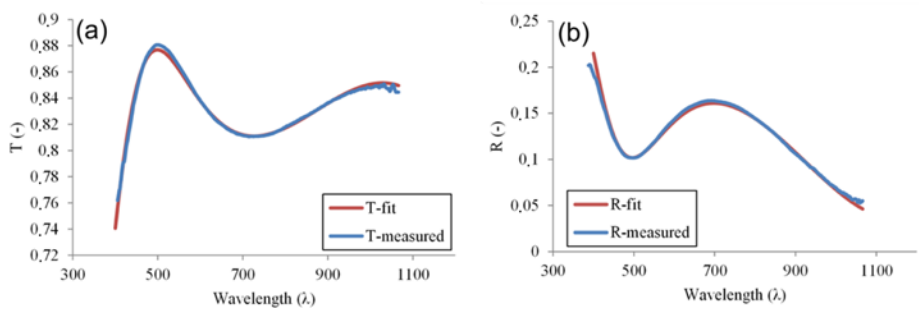

Fig. 7. (a) Measured transmission and fit based on two sub layers modeled with two lorentz oscillators . (b) Measured reflection and fit based on two sub layers modeled with two lorentz oscillators.

ITO-1 thickness is set to 86 nm and for ITO-2 the thickness is set to 36 nm. ITO-1 is located closest to the substrate. The thickness of both ITO layers has been varied to match the simulation data with the experimental planar reference data, after which they remain fixed for the ILE simulations. The organic layer thickness is set to 141 nm as determined by optical interferometry on the planar device. The cathode layer thickness is 100 nm. In both models, the emissive source is placed at a fixed distance of 56 nm from the cathode. For the comparison of the software models with the experimental results of samples with an ILE layer, the simulated planarization layer thickness is set as a variable. The optimal thickness was then selected on the basis of best agreement for peak positions. For the software simulation comparison, the structure shown in Fig. 2 is simplified to a perfectly rectangular shape. The groove track pitch is 600 nm and the structure width is 260 nm. In the comparison between experiment and simulation, the dimensions of the light extraction structure and the height of the groove are varied to compensate for the non-perfect rectangular shape. The optimal structure height was selected on the basis of best agreement for base shape. Simulations and measurements of the light emission are carried out as a function of the inclination angle in the plane that is perpendicular to the groove direction as illustrated in Fig. 2. For both models the unit cell is defined by the structure pitch of 600 nm. The light generation in the OLED is simulated with two dipoles located at 1/8th (75 nm) and 3/8th (225 nm) of the unit cell width and the positions are measured from the middle of the groove. The dipoles are located in the middle of the 20 nm EML layer. In the FDTD model the total OLED width is set to 25 µm for the planar reference OLED and 119.4 µm for the OLED with ILE layer. The mesh accuracy in Lumerical is respectively set to 8 and 4, which is sufficient while having an acceptable computational time. In the RCWA model three coupled diffraction orders are calculated. With a pitch of 600 nm this means that the coupling between all non-evanescent diffraction orders is calculated. A resolution of 100 angles per Brillouin zone is used and calculations are made for wavelengths of 500, 550 and 600 nm. For both simulation methods, the far field angular power distributions are calculated in the substrate medium. As explained previously, this result corresponds to the emission in air when a cylindrical lens is used. By using the cylindrical lens we can neglect (total or partial) internal reflections at the glass/air interface and we do not have to deal with non-coherent contributions entering the OLED from the substrate side.

4. Results

4.1 Characteristics of OLED samples

The integrating sphere measurement results of the planar reference OLED sample as well as the sample with ILE layer are listed in Table 1. The color point of the reference sample is x = 0.321 and y = 0.619. Adding the ILE layer gives a minor difference in color point. The measurements with a hemisphere lens show a 5.6% gain in light directed into the substrate

#203447 - $15.00 USD Received 20 Dec 2013; revised 21 Feb 2014; accepted 26 Feb 2014; published 12 Mar 2014

due to the use of the ILE layer at 2.06 mA/cm^2.The gain at 0.69 mA/cm^2 and 6.87 mA/cm^2 equals 5.8% and 6.8% respectively. Direct comparison of the reference sample and the sample with an ILE layer, without a hemisphere lens, gives a higher gain factor (up to 21%). Note that this additional gain is measured as a result of extracting light from the substrate waveguide modes.

Table 1. Integrating sphere measurements

Sample	Output [lm/cm^2]	Current [mA/cm^2]	Voltage [V]	Power eff. [lm/W]
Planar Reference	0.265	2.06	3.44	37.4
OLED + ILE	0.306	2.06	3.29	45.2
Planar Reference + Hemisphere	0.47	2.06	3.16	72.1
OLED + ILE + Hemisphere	0.49	2.06	3.14	76.2

4.2 Data comparison for the planar reference OLED

The emission of the planar reference OLED has been simulated and measured as a function of the emission angle. The comparison with the FDTD simulation software is made for three wavelengths: 500, 550 and 600 nm (see Fig. 8(a)). For comparison of the experimental data and simulation results the intensity is normalized with respect to the emission in the perpendicular direction (averaged over 0° till 5°). The results obtained through the two software models are compared with experiments and with the analytical solution. The analytical data is calculated from the analytical formulae for cavity emission from planar OLEDs as described in section 2.3. There is excellent agreement between the four different data sets (Fig. 8(a)).

These simulations show that the angular profile depends on the wavelength, which means that a planar white OLED would have a color shift when tilting the sample. The differences found at angles over 75 degrees can be attributed to the fact that the FDTD method requires a limited size of the samples whereas both the RCWA and the analytical solution assume infinite slabs.

4.3 Data comparison for OLEDs with internal light extraction layer

Figure 8(b) shows the measured angular intensity distributions for an OLED with an ILE layer. The non-normalized experimental results at a wavelength of 550 nm illustrate the difference in angular emission profile between the planar reference OLED and the OLED with ILE layer (see Fig. 8(b)). Narrow diffraction peaks are measured at an emission angle of 11.6°, 24.3°, 27.3° and 31.1°. The Fig. shows that for light emitted perpendicular to the grooves no light of 550 nm is gained by adding the internal 2D groove structure.

The emission profile of the OLED with ILE layer is simulated for three wavelengths: 500, 550 and 600 nm (see Fig. 9). The intensity is normalized with respect to the emission in the perpendicular direction (averaged over 0° till 5°). The narrow peaks in the angular emission profile vary with the wavelength, as illustrated in Fig. 10. Due to positive and negative diffraction individual peaks show different wavelength shifts with respect to their emission angle. These shifts are readily observed in the experimental measurements and allow us to attribute individual peaks to specific orders of diffraction. Besides the three wavelengths that are analyzed and compared with simulations, the Angular Spectral Measurements (ASMs) provide data over a large wavelength range, as illustrated in Fig. 11. One can see how the ILE layer introduces narrow peaks at certain angles for different wavelengths.

#203447 - $15.00 USD Received 20 Dec 2013; revised 21 Feb 2014; accepted 26 Feb 2014; published 12 Mar 2014

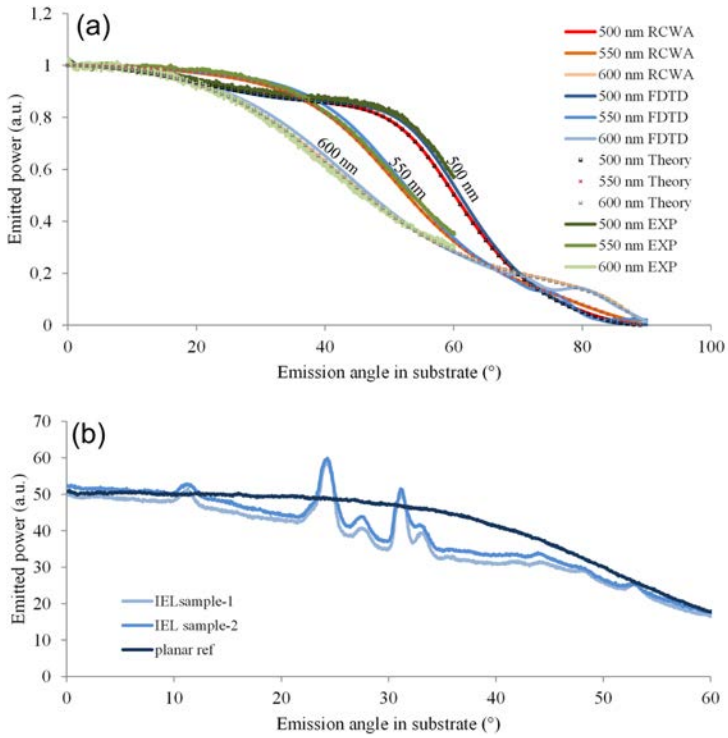

Fig. 8. (a) Emitted intensity versus the emission angle for the planar OLED calculated with RCWA, FDTD as well as with the theoretical formulae and compared with the experimental data. The comparison is made for three different wavelengths (500, 550 and 600 nm) and excellent agreement is observed. (b) Emitted intensity versus the emission angle for two OLEDs with an ILE layer compared with the planar reference sample for a wavelength of 550 nm.

5. Discussion

The RCWA and FDTD methods solve Maxwell's equations in different ways as discussed in sections 2.1 and 2.2 . Therefore, congruity between the simulation results means that the mathematical calculations of both RCWA and FDTD are correct. Congruity with experimental data demonstrates that both software models can accurately describe OLEDs with an ILE layer. The simulation results of the RCWA and FDTD methods are in good agreement with each other for the planar OLED. Moreover, the comparison with the analytical formulae and experimental data show that the mathematical calculations of both software models are correct for a planar OLED. For the OLED with ILE layer the position of the diffraction peaks and intensity distribution match well between the FDTD and the RCWA model. In addition to this, there is a good agreement between simulation results and the experimental angular distribution measurements.

#203447 - $15.00 USD Received 20 Dec 2013; revised 21 Feb 2014; accepted 26 Feb 2014; published 12 Mar 2014

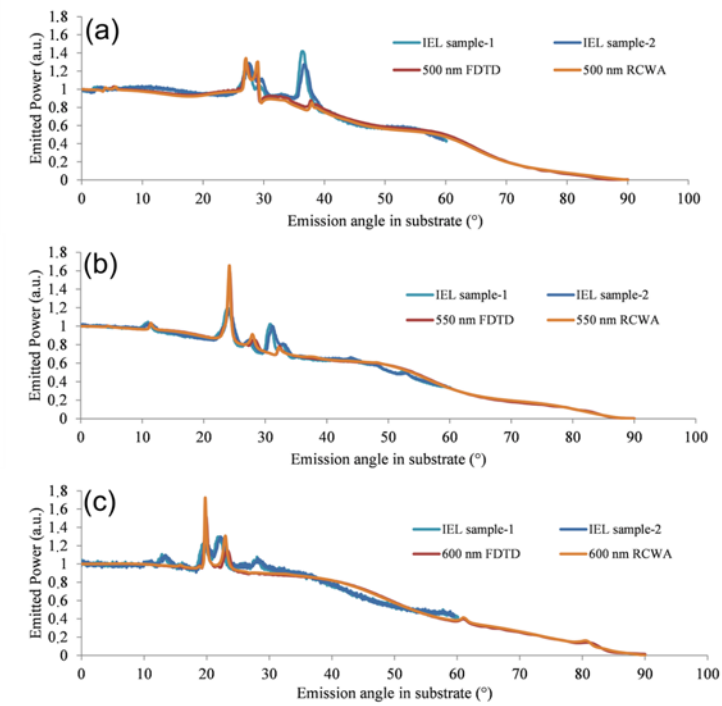

Fig. 9. For three different wavelengths (500, 550 and 600 nm) the angular emission profile of the OLED with ILE layer is compared for simulated (FDTD and RCWA) and experimental data of two samples (sample 1 & 2).

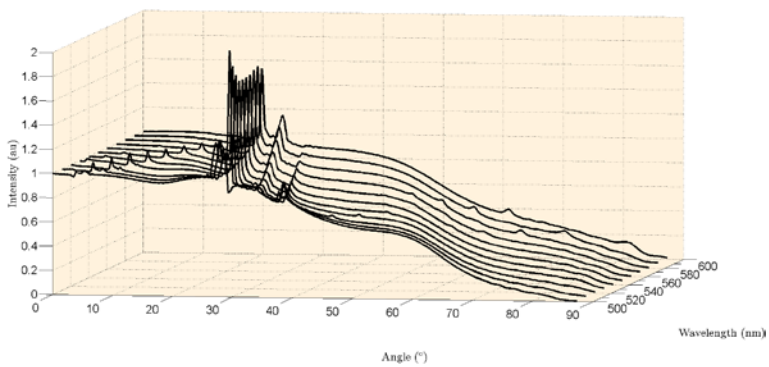

Fig. 10. Angular emission distribution as a function of the wavelength, simulated with the FDTD method.

#203447 - $15.00 USD Received 20 Dec 2013; revised 21 Feb 2014; accepted 26 Feb 2014; published 12 Mar 2014

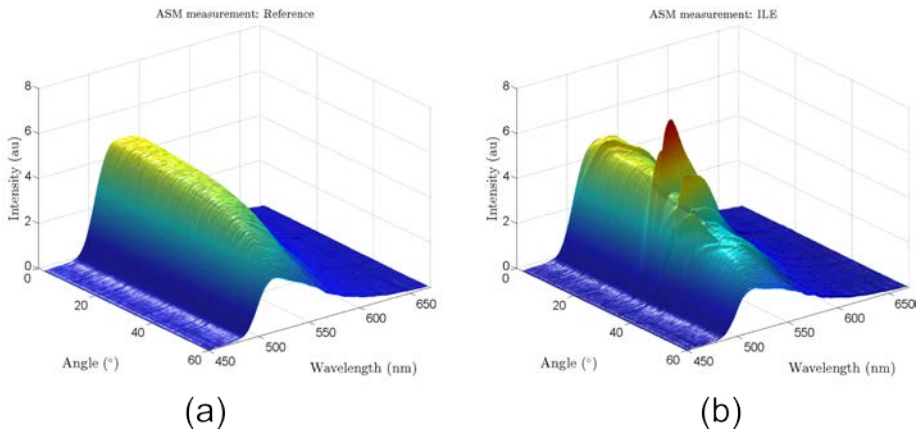

Fig. 11. Angular Spectral Measurement data (ASMs) showing the spectrum of the emitted radiation for different angles as measured in the plane of detection (see Fig. 2) for a reference sample (a) and a sample with ILE (b). The intensity scale in both figures. is identical.

The peak positions and baseline level of the curves are well aligned. The diffraction peaks are slightly broadened, due to limited angular resolution of the measurement setup. Differences in peak height can be explained by process variation. These process variations, resulting in small changes in optical constants and layer thicknesses, combined with limited resolution of the experimental setup prevent a perfect agreement between simulation and experiment. In the comparison of experiment and simulation three fit parameters have been used, namely the ITO layer thickness, planarization thickness and structure height. The ITO layer thickness was fitted by comparing the simulations with experimental data of the planar reference data. The intended 135 nm sputtered layer thickness was simulated with a total thickness of 122 nm. Two layers were used to fit the graded index; ITO-1 was set to 86 nm and ITO-2 was set to 36 nm. The small difference in layer thickness is likely for a sputter process that has not fully matured yet. The planarization thickness is set to 0 nm. Being applied by spin-coating it is possible that the residual planarization layer thickness on top of the grooves is zero due to the high spin speed of 5000 rpm. The structure height has been fitted with a height of 260 nm. This value is lower than the AFM measured value of 290 nm on the master stamper. However, due to shrinkage in the replication process and the fact that in practice the structure is slightly rounded, an average trapezium height of 260 nm is plausible. Simulating the ITO layer with one layer, instead of two layers and thereby altering the optical constants and number of interfaces, is accompanied by small changes in peak position and peak height. Further fine-tuning of the optical constants of the organic stack might improve the peak height correlation between simulation and experiment.

The narrow peaks in Figs. 9, 10 and 11 indicate that the diffractive structure extracts light of the waveguide modes in a specific angular direction. The power contained within these peaks is limited which results in a small increase in light extraction. The baseline shape for the OLED with ILE layer is determined by the OLED cavity effect. Altering the planarization layer thickness changes the position of these local maxima. The shape of the angular distribution is different from that of the planar OLED. The difference in light distribution between the planar OLED and the OLED with ILE layer shows that the light is more forward directed for the internally structured samples, demonstrating the possibilities of radiation pattern shaping by use of internal light management layers.

6. Conclusion

The Lumerical FDTD software has been compared with the CAMFR RCWA software to model a planar and structured OLED. Both software packages use different algorithms to

#203447 - $15.00 USD Received 20 Dec 2013; revised 21 Feb 2014; accepted 26 Feb 2014; published 12 Mar 2014

solve the Maxwell equations. The angular intensity distribution for the planar OLED is in good agreement for both models and matches well with both experiment and theoretical calculations. This result proves that the physical representation of an OLED is correct for both software packages.

The software model matches well with the experimental data of an OLED with ILE layer. This demonstrates that not only the algorithms are correct, but the software model is also a correct representation of the complex OLEDs with ILE layers. These results enable the use of FDTD as well as RCWA software simulations to optically optimize the OLED stack and ILE layers. The models have shown that the structure height, planarization layer thickness and optical constants of the ITO layer are important parameters to optimize light gain. However, it is believed that for this diffractive light management structure, light gain values will remain small.

Acknowledgments

OM&T B.V. would like to thank the Dutch Agentschap.nl (contract INT111033) for funding. The university of Ghent would like to thank the Belgian Agentschap voor innovatie door wetenschap en techniek (contract IWT 120334) for funding.

#203447 - $15.00 USD Received 20 Dec 2013; revised 21 Feb 2014; accepted 26 Feb 2014; published 12 Mar 2014